Published in final edited form as:
J Inherit Metab Dis. 2010 June ; 33(3): 261–270. doi:10.1007/s10545-010-9109-3.

Glycosphingolipid storage leads to the enhanced degradation of the B cell receptor in Sandhoff disease mice

Danielle te Vruchte,
Department of Pharmacology, University of Oxford, Mansfield Road, Oxford OX1 3QT, UK

Aruna Jeans,
Department of Pharmacology, University of Oxford, Mansfield Road, Oxford OX1 3QT, UK

Frances M. Platt, and
Department of Pharmacology, University of Oxford, Mansfield Road, Oxford OX1 3QT, UK

Daniel John Sillence
Cell Signalling Lab, Leicester School of Pharmacy, De Montfort University, The Gateway, Leicester LE1 9BH, UK

Abstract

Glycosphingolipid storage diseases are a group of inherited metabolic diseases in which glycosphingolipids accumulate due to their impaired lysosomal breakdown. Splenic B cells isolated from NPC1, Sandhoff, GM1-gangliosidosis and Fabry disease mouse models showed large (20- to 30-fold) increases in disease specific glycosphingoli-pids and up to a 4-fold increase in cholesterol. The magnitude of glycosphingolipid storage was in the order NPC1 > Sandhoff, ~ GM1 gangliosidosis > Fabry. Except for Fabry disease, glycosphingolipid storage led to an increase in the lysosomal compartment and altered glycosphingolipid trafficking. In order to investigate the consequences of storage on B cell function, the levels of surface expression of B cell IgM receptor and its associated components were quantitated in Sandhoff B cells, since they are all raft-associated on activation. Both the B cell receptor, CD21 and CD19 had decreased cell surface expression. In contrast, CD40 and MHC II, surface receptors that do not associate with lipid rafts, were unchanged. Using a pulse chase biotinylation procedure, surface B cell receptors on a Sandhoff lymphoblast cell line were found to have a significantly decreased half-life. Increased co-localization of fluorescently conjugated cholera toxin and lysosomes was also observed in Sandhoff B cells. Glycosphingolipid storage leads to the enhanced formation of lysosomal lipid rafts, altered endocytic trafficking and increased degradation of the B cell receptor.

Introduction

Glycosphingolipids (GSLs) are clearly vital for the survival of complex organisms (Wandall et al. 2005; Yamashita et al. 1999). Although their functions have yet to be fully elucidated, specific GSLs are important in neuronal and immune function (Kawai et al. 2001; Simpson et al. 2004; Vyas et al. 2002; Zhou et al. 2004). How GSLs perform their roles is not known, but one theory involves the formation of GSL rafts, specialized platforms in the plane of the plasma membrane that are important in signaling and membrane sorting (Simons and van

dsillence@dmu.ac.uk.
Competing interest: None declared.
Communicated by: Douglas A. Brooks

Europe PMC Funders Author Manuscripts

Meer 1988). One example of lipid raft-mediated signaling is the response of B cells when they encounter a specific antigen. B cell receptors (BCR, cell surface antigen receptor) are normally in the liquid-disordered part of the plasma membrane with the inhibitory proteins CD45 and CD22. Following clustering of the B cell receptor by antigen, the receptor, co-receptors CD21 and CD19 are recruited to membrane rafts (Cherukuri et al. 2004). The cytosolic domains of the signaling subunits are then phosphorylated by the raft resident tyrosine kinase *lyn*. Tyrosine phosphates then recruit *Syc* which phosphorylates SHC and a signaling cascade is initiated (Reth and Wienands 1997). In turn, these events lead to an enlarged endoplasmic reticulum and increased antibody production. Since GSLs are thought to be important components of lipid rafts, the effect of GSL storage on the BCR receptor as well as the CD19/CD21 complex was studied.

GSL storage diseases are inherited metabolic diseases in which GSLs accumulate due to their impaired lysosomal catabolism. The majority are autosomal recessive disorders resulting from mutations in the genes that encode the glycohydrolases, which sequentially degrade GSLs in the lysosome. However, GSL storage also occurs in some diseases despite the presence of fully functional glycohydrolases, and in these disorders the storage of GSL occurs secondarily to changes in lipid trafficking (Walkley 2004). One of these disorders is Niemann-Pick type C (NPC) where storage occurs due to defective NPC1, a multimembrane spanning endosomal protein of unknown function (Passeggio and Liscum 2005). In mouse models of NPC as well as other GSL storage diseases, imino sugars that inhibit the synthesis of GSL are an effective therapy (Jeyakumar et al. 1999; Zervas et al. 2001). However, how the storage of GSLs leads to pathology is still an open question. One theory suggests that the accumulation of GSLs and cholesterol leads to the formation of a mislocalized lipid raft in the lysosome of storing cells (Simons and Gruenberg 2000). This could be expected to lead to relocation of lipid raft-associated proteins from the plasma membrane to the lysosome, leading to increased degradation.

Although in the majority of these diseases the pathology is primarily neuronal, the immune system has also been implicated; for example: (1) Increase in inflammatory cytokines and microglial activation in GM1 gangliosidosis, GM2 gangliosidosis, and NPC (Jeyakumar et al. 2003; Mizukami et al. 2002; Wada et al. 2000; Wu et al. 2005; (2) bone marrow transplantation can decrease neuronal loss even though the neurons store more (Jeyakumar et al. 2001; Norflus et al. 1998); (3) Sandhoff mice respond to antiinflammatory drugs (Jeyakumar et al. 2004); (4) genetic deletion of a leukocyte chemokine, MIP-1α, leads to decreased neuronal apoptosis and increased lifespan in Sandhoff disease (Wu and Proia 2004); (5) A Gaucher mouse model shows B cell hyperproliferation (Mizukami et al. 2002); and (6) the immune system is a potential environmental factor that influences clinical heterogeneity (Lachmann et al. 2004a).

In the present study, B cells isolated from the NPC1 (*NPC1*$^{-/-}$), Sandhoff (*Hexb*$^{-/-}$), GM1-gangliosidosis (*β-gal*$^{-/-}$), and Fabry (*α-gal*$^{-/-}$) disease mouse models were found to store electron dense material. Lipid storage was quantitated using HPLC and cholesterol analysis. We found an increase in lysotracker staining and altered BODIPY LacCer trafficking using a pulse labeling protocol. These changes were accompanied by the decreased surface expression of the B cell receptor, as well as the co-receptors CD21 and CD19 (lipid raft-associated proteins) but not CD40 and MHC II, integral membrane proteins that do not associate with lipid rafts. In a Sandhoff patient-derived B cell line, an increased turnover of B cell receptor was observed. When the subcellular distribution of B cell lipid rafts in the endocytic pathway were probed using fluorescent cholera toxin conjugate, increased co-localization with lysotracker was observed in Sandhoff lymphoblasts. These data suggest that the intracellular accumulation of lipid rafts may lead to the mistargeting and degradation of lipid raft-associated B cell receptor. These findings may have implications of how

proteins are sorted in the endocytic pathway and how the accumulation of GSLs may disrupt cell function.

Materials and methods

HPLC grade acetonitrile, methanol, chloroform and butanol were from VWR (Poole, Dorset, UK). Acetone was from Fisher Chemicals (Loughborough, UK). Spurr resin was from Taab Laboratories (Berkshire, UK). TNP-Ficoll was from Biosearch Technologies (Novarto, CA), DPA-BSA and DPA-6S columns were from Supelco (Ballafonte, PA). C_{18} SepPak columns were from Waters (Milford, MA). Ceramide glycanase (E.C. 3.2.1.123) was from Calbiochem (La Jolla, CA). Lysotracker® green was from Invitrogen (Paisley, UK). HRP conjugated anti-mouse IgG, M and A was from Serotec (Kidlington, UK). Immuno Maxisorp plates were from Nunc (Roskilde, Denmark). TMB substrate and Mouse anti-TNP IgG_2 were from Becton Dickinson (Oxford, UK).

Animals

Sandhoff (*Hexb*$^{-/-}$) mice (Yamanaka et al. 1994) were provided by Dr Richard Proia (National Institutes of Health, Bethesda, MD, USA). GM1 gangliosidosis mice (*β-gal*$^{-/-}$) were provided by Dr Alessandra d'Azzo (St Jude Children's Hospital, Memphis, TN, USA). Fabry (*α-gal*$^{-/-}$) mice (Ohshima et al. 1997) were provided by Dr. Ashok Kulkarni (National Institutes of Health, Bethesda, MD, USA). npc1^{NIH} spontaneous mutant mice on the BALB/cJ background (Pentchev et al. 1984) (*NPC1*$^{-/-}$) were provided by Dr Robin Lachmann (Addenbrooke's Hospital, Cambridge, UK) and were maintained by brother-sister mating of heterozygous animals. All mice were bred and housed under standard non-sterile conditions, with food and water available ad lib. All animal studies were conducted using protocols approved by the UK Home Office (Animals Scientific Procedures Act, 1986). Table 1 gives a summary of the mouse models used in the study.

Electron microscopy

Cells for electron microscopy (~10^7 cells) were washed in PBS and fixed in 2% paraformaldehyde/2% gluteraldehyde in PBS overnight at 4°C. After washing 4 times in PBS, cells were post-fixed with 1% osmium tetroxide for 1 h at room temperature. After washing in ultrapure water, samples were dehydrated through an ethanol series and embedded in spurr resin. Once embedded, 80-nm ultrathin sections were cut using a Reichart ultracut E ultramicrotome and collected onto formvar coated grids. Sections were stained for 5 min in 2% alcoholic UA (uranyl acetate) followed by 15 min in Reynold's lead citrate and observed with a Joel JEM 1010 microscope at 80 kV.

Purification of GSLs for HPLC

GSLs were extracted by addition of 3.2 vol of $CHCl_3$/MeOH (1:2.2) for 10 min at room temperature (Bligh and Dyer 1959; te Vruchte et al. 2004). GSLs were then purified by silicic acid chromatography (Dasgupta and Hogan 2001). Silicic acid columns were pre-equilibrated in $CHCl_3$ and the samples were loaded onto the column and washed with 6 mls of $CHCl_3$. Cholesterol was eluted with 10 ml $CHCl_3$/MeOH (49:1). GSLs were eluted with 10 ml MeOH and the eluates dried under nitrogen.

Quantitation of GSL oligosaccharides by HPLC

GSLs were analyzed according to Neville (Neville et al. 2004) with the following modifications. Dried lipid extracts were resuspended in 10 μl incubation buffer (1 mg/ml sodium deoxytaurocholate in 50 mM sodium acetate pH 5.0). After vigorous vortexing and spinning in a benchtop picofuge, 10 μl of 50 mU/10 μl of ceramide glycanase in incubation

buffer was added to release glycans. Glucosylceramide is only partially digested due to the specificity of the glycanase (Wing et al. 2001). After 18 h, 10 µl of water was added to each enzyme digest followed by 80 µl of anthranilic acid (30 mg/ml) and sodium cyanoborohydride (45 mg/ml) in 4% $NaCOOCH_3.3H_2O$, 3% H_3BO_4 in MeOH to each digest and incubated for 1 h at 80°C. Derivatized oligosaccharides were purified on DPA-6S columns pre-equilibrated with 2 × 1 ml CH_3CN. 1 ml 97:3 $CH_3CN:H_2O$ was added to each sample and vortexed prior to loading. Columns were washed with 4×1 ml 99:1 $CH_3CN:H_2O$ and then with 0.5 ml 97:3 $CH_3CN:H_2O$ and the derivatized oligosaccharides were eluted with 2×0.6 ml water into screw-cap eppendorfs and stored at 4°C in the dark until ready for NP-HPLC, using a Waters Alliance 2695 separations module, an in-line Waters 474 fluorescence detector separation and a 4.6×250 mm TSK gel-Amide 80 column (Anachem, Luton, UK).

Quantitation of cholesterol

Cholesterol was quantitated using a method similar to that of Franey (Franey and Amador 1968). Samples were resuspended in 50 µl EtOH and transferred to a microtitre plate along with cholesterol standards (1 mg/ml in EtOH) in duplicate and dried briefly at 80°C. After the addition of 75 µl of 3 mM $FeCl_3.6H_20$ in glacial acetic acid and 50 µl concentrated H_2SO_4, the plate was incubated for 10 min in the dark and the absorbance read at 570 nm.

Isolation of splenic B lymphocytes

B lymphocytes were separated from mononuclear cells prepared from spleen cell suspensions using MACS CD19 MicroBeads (Miltenyi Biotec, Surrey, UK) according to the manufacturer's instructions.

Lysotracker® staining and quantification

Lysotracker quantification was performed as described (Lachmann et al. 2004b). Isolated B cells were incubated with 200 nM Lysotracker® green for 10 min in the dark at room temperature, centrifuged at 2,000g for 1 min in a Heraeus Biofuge A desktop centrifuge and resuspended in 0.5 ml of PBS. After running on a Beckton Dickinson FACScan flow cytometer, analysis was performed using CellQuest software.

Assessment of BODIPY-LacCer trafficking

Isolated B lymphocytes were pulse-labelled with 13 µM BODIPY-LacCer for 1 h followed by a 90-min chase in medium containing 10% FCS and observed using a Zeiss Axioplan 2 fluorescence microscope as described previously (Sillence et al. 2002).

Flow cytometry

Diced mouse spleens were forced through a 70µm nylon mesh. Erythrocytes were lysed with lysis buffer (140 mM NH_4Cl, 17 mM Tris pH 7.2). Cells were stained with anti-CD19 PE, MHC II-FITC, CD21-FITC, IgM-FITC in FACS buffer (0.1% BSA, 0.02M NaN_3 in PBS), for 30 min on ice. Cells were washed with 10% BSA, followed by a FACS buffer wash. Cells were resuspended in 0.4ml FACS buffer, and samples run on a FACScalibur. CellQuest was used to analyze the data.

Assessment of cholera toxin trafficking

B lymphoblasts were labeled with 5 µg/ml of FITC-cholera toxin for 2 h. Then, 4 µM lysotracker red was added for the last 15 min. Cells were washed with PBS before viewing under a Leica confocal fluorescence microscope.

Surface biotinylation

The protocol was identical to (Tian et al. 2004) with the following changes. Human B lymphoblasts were surface biotinylated and then chased in the presence of bovine cross-reacted 10 μg/ml anti-IgM and IgG (Jackson labs). Cells were then lysed and the B cell receptor was immunoprecipitated and quantitated by western blotting using an anti-Biotin antibody (Vectorlabs).

Results

B cells from storage disease mice contain electron dense material

We aimed to study the mechanisms by which GSL storage disrupts cell function by studying a primary cell type isolated from diseased mice. Electron microscopy of B cells derived from the spleen of storage disease mouse models revealed increases in cytoplasmic volume and round translucent organelles resembling lysosomes (Fig. 1a, C57Bl/6 and Fig. 1e, Balb/C, $NPC1^{+/+}$). In Fabry disease B cells (Fig. 1b, α-$Gal^{-/-}$) and Sandhoff disease (Fig. 1d, β-$Hexb^{-/-}$), electron dense material is associated with the periphery of the storage bodies. In GM1 gangliosidosis (Fig. 1c, β-$Gal^{-/-}$) and NPC (Fig. 1f, $NPC1^{-/-}$), large vacuolar structures with electron dense inclusions were present. Since the GSL composition of storing B cells had not been previously analyzed, we characterized the storage material using sensitive biochemical assays.

GSL and cholesterol storage in splenic B cells

Normal B cells from C57Bl/6 and Balb/c ($NPC1^{+/+}$) mice express similar GSLs including LacCer, Globosides (Gb3 and Gb4) as well as mono and disialylated gangliosides such as GM1, GM2, and GD1 (Table 2; abbreviations defined in footnote to table). Balb/c mice additionally express GM3. The GSL composition is similar to that of B cell hybridomas (Ugorski et al. 1984) and B cells isolated from CBA/J mice (Portner et al. 1993). B cells isolated from storage disease mice show disease-specific changes in GSL composition. In α-$gal^{-/-}$(Fabry model) mice, Gb3 increases by 30-fold. In β-$gal^{-/-}$(GM1-gangliosidosis model) mice ~3-fold increases were found in GM1 and 20-fold increases in GA1 (Table 2). Similarly in β-$Hexb^{-/-}$ (Sandhoff model) desialylated GM2 (GA2) is the main storage product (20-fold). Desialylated GSLs occur via a sialidase, particularly active in mice (Sango et al. 1995). In $NPC1^{-/-}$, a broader range of GSL accumulation occurs, increases in LacCer (~7 fold), GM3 (20-fold) and GM2 (4-fold), globosides (4-fold) and complex gangliosides (~2-fold). Since the relative abundance of different GSLs varies (Table 2), the total level of GSL storage also varies (Table 3). Overall, the increases in total GSLs were largest in $NPC1^{-/-}$ (4-fold) > β-$Gal^{-/-}$ ~ β-$Hexb^{-/-}$ (2.5-fold) > α-$Gal^{-/-}$ (1.8 fold). Increases in disease-specific GSLs led to increases in total cholesterol levels. In many instances, cholesterol storage was in excess of the total level of GSL storage. Overall increases in cholesterol levels were largest in $NPC1^{-/-}$ and β-$Hexb^{-/-}$ (~4-fold)> β-$Gal^{-/-}$ (~2-fold)> α-$Gal^{-/-}$ (~1.8-fold) (Table 3). Next, we investigated the consequences of lipid storage.

Lysosomal compartment expansion in storing B cells

GSL and cholesterol storage may result in changes in lysosomal burden. LysoTracker probes are cell permeable, that fluoresce at acidic pH and may be used for labeling lysosomes and late endosomes. Using this probe, labeling of the acidic compartments increases in the diseased cells in the order $NPC1^{-/-}$~β-$Gal^{-/-}$ (~3-fold) > β-$Hexb^{-/-}$ (~2-fold) > α-$Gal^{-/-}$ (no increase) (Table 3), correlating with the level of GSL storage as shown in Table 2.

Europe PMC Funders Author Manuscripts

GSL storing B cells accumulate BODIPY-LacCer in endocytic structures

In fibroblasts, BODIPY-LacCer is internalized by a caveolae (lipid raft) pathway of unknown function (Sharma et al. 2004; Singh et al. 2003). Storage disrupts this pathway in fibroblasts (Chen et al. 1999) and now we show altered endocytic targeting in B cells isolated from diseased mice. When normal skin fibroblasts are pulse-labeled with BODIPY-LacCer, the fluorescent lipid targets the Golgi complex (Choudhury et al. 2002). In B cells isolated from normal mice, BODIPY-LacCer pulse labeling also leads to a perinuclear distribution consistent with Golgi targeting (Fig. 2). Storing splenic B cells show increases in BODIPY-LacCer trafficking to punctate endocytic structures in the order $NPC1^{-/-} \sim \beta\text{-}Gal^{-/-} > \beta\text{-}Hexb^{-/-} > \alpha\text{-}Gal^{-/-}$ (Table 4). In some storing B cells, morphological changes occur, $NPC1^{-/-}$B cells show large punctate structures that may relate to the large inclusions seen by electron microscopy (Fig. 1). So far, the consequences of altered lipid-raft function are not described, we determined the effects of storage on surface expression of B cell receptors

GSL storage decreases the surface expression of the B cell surface antigen receptor

Previous studies have shown GSL-dependent mislocalization of the lipid raft-associated protein annexin 2 from early to late endosomes in NPC cell culture models (te Vruchte et al. 2004). Increased degradation is predicted by the ‘mislocalization hypothesis’ (Sillence and Platt 2004; Simons and Gruenberg 2000) due to the trapping of lipid raft components in lysosomes. If correct, the B cell receptor would be expected to show reduced surface expression. Consistent with the hypothesis, storage results in a reduction in the expression of the BCR and its lipid raft-targeting components CD21 (~20% reduction, t test $p < 0.01$) and CD19 (10% reduction, t test $p < 0.05$) (Fig. 3). In contrast, CD40 and MHC II do not associate with lipid rafts (Malapati and Pierce 2001; Karacsonyi et al. 2005) or show reduced surface expression (Fig. 3), consistent with specific effects on lipid raft components (2-way ANOVA $p < 0.05$). In addition, the surface expression of the B cell antigen receptor was quantitated on normal and Sandhoff patient EBV-transformed B lymphoblasts (Maret et al. 1985). Sandhoff lymphoblasts showed, ~60% decrease in sIgG surface levels (Fig. 3). Due to the ready availability of large quantities of B lymphoblasts, we studied the effects storage on the endocytic distribution of lipid rafts and the turnover of the B cell antigen receptor on these cells.

Storing cells show redistribution of GM1

In order to investigate the distribution of GM1 in the endosomal pathway, cholera toxin was used as a probe (Harder et al. 1998). Pulse labeling of normal B lymphoblasts with FITC labeled cholera toxin (green) shows a perinuclear distribution similar to the Golgi (Schapiro et al. 1998) (Fig. 4a). In normal cells, the fluorescence does not overlap with the lysotracker staining (Fig. 4b). In B cells isolated from a Sandhoff patient, increases in the number lysotracker-labeled structures are seen (Fig. 4b vs e). In Sandhoff lymphoblasts, an increase in the co-localization of cholera toxin and lysotracker occurs, as can be seen from the merged image (Fig. 4f). This is consistent with an increase in the level of lysosomal GM1 even in $\beta\text{-}Hexb^{-/-}$-deficient cells that store GM2. This is consistent with the hypothesis that raft-associated lipids are redistributed on storage.

GSL storage increases the turnover of the B cell receptor

If lipid raft-associated proteins are also mislocalized to lysosomes on storage, the B cell receptor may be expected to have an increased rate of degradation in $\beta\text{-}Hexb^{-/-}$-deficient cells. Using a pulse chase biotinylation assay, the B cell receptor on normal human B lymphoblasts did not turn over significantly during the 4-h period of the study. In contrast,

the B cell receptor on human Sandhoff B lymphoblasts was found to turnover more rapidly with a half-life of 3 h (Fig. 5) consistent with increased degradation.

Discussion

Previously, it has been shown that a cell culture model of NPC1 disease has GSL-dependent disruption of endocytic sorting (te Vruchte et al. 2004). The present results show that primary B cells isolated from an NPC1 mouse model, as well as mouse models of other GSL storage diseases, also show altered endocytic sorting. Moreover, in Sandhoff B cells, cholera toxin (a GM1 binding toxin) shows altered trafficking from the Golgi to lysosomes and the B cell receptor shows decreased cell surface expression due to an increase in degradation. The present results suggest that GSL storage causes the altered distribution of lipid rafts in β-*Hexb*$^{-/-}$-deficient cells. Endocytic rafts are usually degraded to cholesterol and sphingosine by lysosomal hydrolases; when this process is blocked, both raft-associated lipids and proteins may become trapped, increasing their rate of degradation.

There is increasing evidence for the disruption of lipid raft-associated proteins in GSL storage diseases. T cells isolated from a mouse model of Niemann-Pick type A disease (sphingomyelin and GSLs are stored) show perturbation of lipid rafts and disruption of T cell receptor signaling (Nix and Stoffel 2000). In primary kidney cells isolated from a mouse model of metachromatic leukodystrophy (sulphatide is stored), the lipid raft-associated protein MAL is mislocalized to lysosomes and down-regulated (Saravanan et al. 2004).

Glycolipid rafts have been visualized within endosomal buds (Sharma et al. 2003) an observation that may be related to the preferential localization of GM1 to buds and tubules of high curvature in vitro (Roux et al. 2005). Endosomes sort lipids on the basis of their fluidity (Mukherjee et al. 1999) and GSL storage may disrupt this process by increasing the liquid ordered phase within endosomes. The redistribution of lipid raft components to the lysosome in storing cells may inhibit specific endocytic mechanisms that are necessary for transport to the Golgi (Puri et al. 2001). The present results suggest that altered lipid sorting may also have implications for the sorting of specific proteins.

In B cells, the mass of cholesterol storage is much greater than that of GSLs (present data). Possibly, the accumulation of GSL inhibits cholesterol removal from endosomes to the ER where it is esterified, possibly by inhibiting the function of NPC1 (Puri et al. 1999). In contrast, in α-*Gal*$^{-/-}$(Fabry) mice, despite increased Gb3, no large increases in cholesterol potentially reflecting GSL specificity occurred either in NPC1 redistribution and/or raft formation. In addition, Fabry mice show no increases in lysotracker staining or altered BODIPY LacCer distribution, possibly reflecting the lower level of storage in comparison to the other diseases. Possibly, GSL storage is tolerated up to a certain level. Previously, the level of GSL storage found in Gaucher fibroblasts was not sufficient to disrupt endocytosis, unless further storage was induced (Sillence et al. 2002). A critical role for cholesterol storage in altered endocytic sorting has been described (Puri et al. 1999).

In *NPC1*$^{-/-}$ and *Hexb*$^{-/-}$ mice, a lysosomal neuraminidase acts on stored GM2 leading to increases in GA2 at the expense of GM2. In *NPC1*$^{-/-}$ B cells, GM2 is not converted to GA2 as it is in β-*Hexb*$^{-/-}$. Potential reasons for this difference include (1) the subcellular distribution of GM2 is different, and (2) the GM2 storing compartment in *NPC1*$^{-/-}$ B cells is either negative for neuraminidase or is inhibited in some way as a result of the NPC1. In contrast to Hexb$^{-/-}$ B cells, B lymphoblasts from Hexb$^{-/-}$ patients stored Gb4 (~700 pmol/mg protein) instead of GA2 (~800 pmol/mg) as seen in the mouse. Differences in the type of GSL stored may explain why the surface expression of the BCR in the patient-derived Hexb$^{-/-}$ B lymphoblasts was less than that observed for the mouse-derived Hexb$^{-/-}$ B cells

(60% reduction vs 20% reduction, respectively; Fig. 3). This interesting observation suggests that different GSL stored may have consequences for the degradation of the BCR possibly through specific raft formation.

Apart for lipid rafts, GSL storage may also cause disease by other mechanisms. Toxic lyso derivatives may escape the lysosome-disrupting protein activity (Im et al. 2001; Suzuki 1998). Storage may disrupt cation channels that are necessary for late endosomal trafficking and fusion (LaPlante et al. 2002; Pryor et al. 2000; Vanweert et al. 1995). Storage may spread, disrupting cation channels in the ER and receptors at the cell surface (Blom et al. 2001; Pelled et al. 2003; Tessitore et al. 2004; Yu et al. 2005). It has been speculated that storage may lead to mechanical stress via the increase and number and volume of lysosomes (Desnick et al. 1976). Finally, GSL storage leads to a relatively large increase in cholesterol levels that may directly disrupt the function of specific proteins that are sensitive to large-scale changes in membrane fluidity. In order to place these mechanisms in order of importance, it will be necessary to determine how GSLs mediate their functions and to what extent stored material escapes the lysosome.

This study highlights the fact that storage may alter the cell surface expression of immunoreceptors and thus alter immune responses. As this may contribute to clinical heterogeneity, further studies are required to determine the functional consequences of GSL storage on the multiple effector cell types of the immune system.

Acknowledgments

Action Medical Research and the Ara Parseghian Foundation for Medical Research funded this study. The flow cytometry instrument was funded by The Wellcome Trust (084631).

References

Bligh EG, Dyer WJ. A rapid method of total lipid extraction and purification. Can J Biochem Physiol. 1959; 37:911–917. [PubMed: 13671378]

Blom TS, Koivusalo M, Kuismanen E, Kostiainen R, Somerharju P, Ikonen E. Mass spectrometric analysis reveals an increase in plasma membrane polyunsaturated phospholipid species upon cellular cholesterol loading. Biochemistry. 2001; 40:14635–14644. [PubMed: 11724577]

Chen CS, Patterson MC, Wheatley CL, O'Brien JF, Pagano RE. Broad screening test for sphingolipid-storage diseases. Lancet. 1999; 354:901–905. [PubMed: 10489949]

Cherukuri A, Shoham T, Sohn HW, Levy S, Brooks S, Carter R, Pierce SK. The tetraspanin CD81 is necessary for partitioning of coligated CD19/CD21-B cell antigen receptor complexes into signaling-active lipid rafts. J Immunol. 2004; 172:370–380. [PubMed: 14688345]

Choudhury A, Dominguez M, Puri V, Sharma DK, Narita K, Wheatley CL, Marks DL, Pagano RE. Rab proteins mediate Golgi transport of caveola-internalized glycosphingolipids and correct lipid trafficking in Niemann-Pick C cells. J Clin Invest. 2002; 109:1541–1550. [PubMed: 12070301]

Dasgupta S, Hogan EL. Chromatographic resolution and quantitative assay of CNS tissue sphingoids and sphingolipids. J Lipid Res. 2001; 42:301–308. [PubMed: 11181761]

Desnick RJ, Thorpe SR, Fiddler MB. Toward enzyme therapy for lysosomal storage diseases. Physiol Rev. 1976; 56:57–99. [PubMed: 813242]

Franey RJ, Amador E. Serum cholesterol measurement based on ethanol extraction and ferric chloride-sulfuric acid. Clin Chim Acta. 1968; 21:255–263. [PubMed: 4875434]

Harder T, Scheiffele P, Verkade P, Simons K. Lipid domain structure of the plasma membrane revealed by patching of membrane components. J Cell Biol. 1998; 141:929–942. [PubMed: 9585412]

Im DS, Heise CE, Nguyen T, O'Dowd BF, Lynch KR. Identification of a molecular target of psychosine and its role in globoid cell formation. J Cell Biol. 2001; 153:429–434. [PubMed: 11309421]

Jeyakumar M, Butters TD, Cortina-Borja M, Hunnam V, Proia RL, Perry VH, Dwek RA, Platt FM. Delayed symptom onset and increased life expectancy in Sandhoff disease mice treated with N-butyldeoxynojirimycin. Proc Natl Acad Sci USA. 1999; 96:6388–6393. [PubMed: 10339597]

Jeyakumar M, Norflus F, Tifft CJ, Cortina-Borja M, Butters TD, Proia RL, Perry VH, Dwek RA, Platt FM. Enhanced survival in Sandhoff disease mice receiving a combination of substrate deprivation therapy and bone marrow transplantation. Blood. 2001; 97:327–329. [PubMed: 11133779]

Jeyakumar M, Thomas R, Elliot-Smith E, Smith DA, Van Der Spoel AC, D'Azzo A, Hugh Perry V, Butters TD, Dwek RA, Platt FM. Central nervous system inflammation is a hallmark of pathogenesis in mouse models of GM1 and GM2 gangliosidosis. Brain. 2003; 126:974–987. [PubMed: 12615653]

Jeyakumar M, Smith DA, Williams IM, Borja MC, Neville DC, Butters TD, Dwek RA, Platt FM. NSAIDs increase survival in the Sandhoff disease mouse: synergy with N-butyldeoxynojirimycin. Ann Neurol. 2004; 56:642–649. [PubMed: 15505823]

Karacsonyi C, Bedke T, Hinrichsen N, Schwinzer R, Lindner R. MHC II molecules and invariant chain reside in membranes distinct from conventional lipid rafts. J Leukoc Biol. 2005; 78:1097–1105. [PubMed: 16204642]

Kawai H, Allende ML, Wada R, Kono M, Sango K, Deng C, Miyakawa T, Crawley JN, Werth N, Bierfreund U, Sandhoff K, Proia RL. Mice expressing only monosialoganglioside GM3 exhibit lethal audiogenic seizures. J Biol Chem. 2001; 276:6885–6888. [PubMed: 11133999]

Lachmann RH, Grant IR, Halsall D, Cox TM. Twin pairs showing discordance of phenotype in adult Gaucher's disease. Q J Med. 2004a; 97:199–204.

Lachmann RH, te Vruchte D, Lloyd-Evans E, Reinkensmeier G, Sillence DJ, Fernandez-Guillen L, Dwek RA, Butters TD, Cox TM, Platt FM. Treatment with miglustat reverses the lipidtrafficking defect in Niemann-Pick disease type C. Neurobiol Dis. 2004b; 16:654–658. [PubMed: 15262277]

LaPlante JM, Falardeau J, Sun M, Kanazirska M, Brown EM, Slaugenhaupt SA, Vassilev PM. Identification and characterization of the single channel function of human mucolipin-1 implicated in mucolipidosis type IV, a disorder affecting the lysosomal pathway. FEBS Lett. 2002; 532:183–187. [PubMed: 12459486]

Malapati S, Pierce SK. The influence of CD40 on the association of the B cell antigen receptor with lipid rafts in mature and immature cells. Eur J Immunol. 2001; 31:3789–3797. [PubMed: 11745400]

Maret A, Salvayre R, Radon J, Hardy M, Vuillaume M, Lenoir G, Douste-Blazy L. Validity of lymphoid cell line for enzymatic studies of GM2-gangliosidosis variant 0 (Sandhoff disease). Enzyme. 1985; 34:48–56. [PubMed: 3002784]

Mizukami H, Mi Y, Wada R, Kono M, Yamashita T, Liu Y, Werth N, Sandhoff R, Sandhoff K, Proia RL. Systemic inflammation in glucocerebrosidase-deficient mice with minimal glucosylceramide storage. J Clin Invest. 2002; 109:1215–1221. [PubMed: 11994410]

Mukherjee S, Soe TT, Maxfield FR. Endocytic sorting of lipid analogues differing solely in the chemistry of their hydrophobic tails. J Cell Biol. 1999; 144:1271–1284. [PubMed: 10087269]

Neville DCA, Coquard V, Priestman DA, te Vruchte DJM, Sillence DJ, Dwek RA, Platt FM, Butters TD. Analysis of fluorescently labeled glycosphingolipid-derived oligosaccharides following ceramide glycanase digestion and anthranilic acid labeling. Anal Biochem. 2004; 331:275–282. [PubMed: 15265733]

Nix M, Stoffel W. Perturbation of membrane microdomains reduces mitogenic signaling and increases susceptibility to apoptosis after T cell receptor stimulation. Cell Death Differ. 2000; 7:413–424. [PubMed: 10800075]

Norflus F, Tifft CJ, McDonald MP, Goldstein G, Crawley JN, Hoffmann A, Sandhoff K, Suzuki K, Proia RL. Bone marrow transplantation prolongs life span and ameliorates neurologic manifestations in Sandhoff disease mice. J Clin Invest. 1998; 101:1881–1888. [PubMed: 9576752]

Ohshima T, Murray GJ, Swaim WD, Longenecker G, Quirk JM, Cardarelli CO, Sugimoto Y, Pastan I, Gottesman MM, Brady RO, Kulkarni AB. alpha-Galactosidase A deficient mice: a model of Fabry disease. Proc Natl Acad Sci USA. 1997; 94:2540–2544. [PubMed: 9122231]

Passeggio J, Liscum L. Flux of fatty acids through NPC1 lysosomes. J Biol Chem. 2005; 280:10333–10339. [PubMed: 15632139]

Pelled D, Lloyd-Evans E, Riebeling C, Jeyakumar M, Platt FM, Futerman AH. Inhibition of Calcium Uptake via the Sarco/Endoplasmic Reticulum Ca2+-ATPase in a Mouse Model of Sandhoff Disease and Prevention by Treatment with N-Butyldeoxynojirimycin. J Biol Chem. 2003; 278:29496–29501. [PubMed: 12756243]

Pentchev PG, Boothe AD, Kruth HS, Weintroub H, Stivers J, Brady RO. A genetic storage disorder in BALB/C mice with a metabolic block in esterification of exogenous cholesterol. J Biol Chem. 1984; 259:5784–5791. [PubMed: 6325448]

Portner A, Peterkatalinic J, Brade H, Unland F, Buntemeyer H, Muthing J. Structural Characterization of Gangliosides from Resting and Endotoxin-Stimulated Murine B-Lymphocytes. Biochemistry. 1993; 32:12685–12693. [PubMed: 8251488]

Pryor PR, Mullock BM, Bright NA, Gray SR, Luzio JP. The role of intraorganellar Ca(2+) in late endosome-lysosome heterotypic fusion and in the reformation of lysosomes from hybrid organelles. J Cell Biol. 2000; 149:1053–1062. [PubMed: 10831609]

Puri V, Watanabe R, Dominguez M, Sun X, Wheatley CL, Marks DL, Pagano RE. Cholesterol modulates membrane traffic along the endocytic pathway in sphingolipid-storage diseases. Nat Cell Biol. 1999; 1:386–388. [PubMed: 10559968]

Puri V, Watanabe R, Singh RD, Dominguez M, Brown JC, Wheatley CL, Marks DL, Pagano RE. Clathrin-dependent and-independent internalization of plasma membrane sphingolipids initiates two Golgi targeting pathways. J Cell Biol. 2001; 154:535–548. [PubMed: 11481344]

Reth M, Wienands J. Initiation and processing of signals from the B cell antigen receptor. Annu Rev Immunol. 1997; 15:453–479. [PubMed: 9143696]

Roux A, Cuvelier D, Nassoy P, Prost J, Bassereau P, Goud B. Role of curvature and phase transition in lipid sorting and fission of membrane tubules. EMBO J. 2005; 24:1537–1545. [PubMed: 15791208]

Sango K, Yamanaka S, Hoffmann A, Okuda Y, Grinberg A, Westphal H, McDonald MP, Crawley JN, Sandhoff K, Suzuki K, et al. Mouse models of Tay-Sachs and Sandhoff diseases differ in neurologic phenotype and ganglioside metabolism. Nat Genet. 1995; 11:170–176. [PubMed: 7550345]

Saravanan K, Schaeren-Wiemers N, Klein D, Sandhoff R, Schwarz A, Yaghootfam A, Gieselmann V, Franken S. Specific downregulation and mistargeting of the lipid raft-associated protein MAL in a glycolipid storage disorder. Neurobiol Dis. 2004; 16:396–406. [PubMed: 15193296]

Schapiro FB, Lingwood C, Furuya W, Grinstein S. pH-independent retrograde targeting of glycolipids to the Golgi complex. Am J Physiol. 1998; 274:C319–C332. [PubMed: 9486120]

Sharma DK, Choudhury A, Singh RD, Wheatley CL, Marks DL, Pagano RE. Glycosphingolipids internalized via caveolar-related endocytosis rapidly merge with the clathrin pathway in early endosomes and form microdomains for recycling. J Biol Chem. 2003; 278:7564–7572. [PubMed: 12482757]

Sharma DK, Brown JC, Choudhury A, Peterson TE, Holicky E, Marks DL, Simari R, Parton RG, Pagano RE. Selective Stimulation of Caveolar Endocytosis by Glycosphingolipids and Cholesterol. Mol Biol Cell. 2004; 15:3114–3122. [PubMed: 15107466]

Sillence DJ, Platt FM. Glycosphingolipids in endocytic membrane transport. Semin Cell Dev Biol. 2004; 15:409–416. [PubMed: 15207831]

Sillence DJ, Puri V, Marks DL, Butters TD, Dwek RA, Pagano RE, Platt FM. Glucosylceramide modulates membrane traffic along the endocytic pathway. J Lipid Res. 2002; 43:1837–1845. [PubMed: 12401882]

Simons K, Gruenberg J. Jamming the endosomal system: lipid rafts and lysosomal storage diseases. Trends Cell Biol. 2000; 10:459–462. [PubMed: 11050411]

Simons K, van Meer G. Lipid sorting in epithelial cells. Biochemistry. 1988; 27:6197–6202. [PubMed: 3064805]

Simpson MA, Cross H, Proukakis C, Priestman DA, Neville DC, Reinkensmeier G, Wang H, Wiznitzer M, Gurtz K, Verganelaki A, Pryde A, Patton MA, Dwek RA, Butters TD, Platt FM, Crosby AH. Infantile-onset symptomatic epilepsy syndrome caused by a homozygous loss-of-function mutation of GM3 synthase. Nat Genet. 2004; 36:1225–1229. [PubMed: 15502825]

Singh RD, Puri V, Valiyaveettil JT, Marks DL, Bittman R, Pagano RE. Selective Caveolin-1-dependent Endocytosis of Glyco-sphingolipids. Mol Biol Cell. 2003; 14:3254–3265. [PubMed: 12925761]

Suzuki K. Twenty five years of the “psychosine hypothesis”: a personal perspective of its history and present status. Neurochem Res. 1998; 23:251–259. [PubMed: 9482237]

Tessitore A, Del PMM, Sano R, Ma Y, Mann L, Ingrassia A, Laywell ED, Steindler DA, Hendershot LM, D’Azzo A. G(M1)-ganglioside-mediated activation of the unfolded protein response causes neuronal death in a neurodegenerative gangliosidosis. Mol Cell. 2004; 15:753–766. [PubMed: 15350219]

te Vruchte D, Lloyd-Evans E, Veldman RJ, Neville DCA, Dwek RA, Platt FM, van Blitterswijk WJ, Sillence DJ. Accumulation of Glycosphingolipids in Niemann-Pick C Disease Disrupts Endosomal Transport. J Biol Chem. 2004; 279:26167–26175. [PubMed: 15078881]

Tian G, Wilcockson D, Perry VH, Rudd PM, Dwek RA, Platt FM, Platt N. Inhibition of alpha-glucosidases I and II increases the cell surface expression of functional class A macrophage scavenger receptor (SR-A) by extending its half-life. J Biol Chem. 2004; 279:39303–39309. [PubMed: 15234963]

Ugorski M, Nilsson B, Schroer K, Cashel JA, Zopf D. Gas chromatography/mass spectrometry analysis of oligosaccharides from neutral glycosphingolipids of murine B cell hybridomas. J Biol Chem. 1984; 259:481–486. [PubMed: 6608522]

Vanweert AWM, Dunn KW, Geuze HJ, Maxfield FR, Stoorvogel W. Transport from late endosomes to lysosomes, but not sorting of integral membrane proteins in endosomes, depends on the vacuolar proton pump. J Cell Biol. 1995; 130:821–834. [PubMed: 7642700]

Vyas AA, Patel HV, Fromholt SE, Heffer-Lauc M, Vyas KA, Dang J, Schachner M, Schnaar RL. Gangliosides are functional nerve cell ligands for myelin-associated glycoprotein (MAG), an inhibitor of nerve regeneration. Proc Natl Acad Sci USA. 2002; 99:8412–8417. [PubMed: 12060784]

Wada R, Tifft CJ, Proia RL. Microglial activation precedes acute neurodegeneration in Sandhoff disease and is suppressed by bone marrow transplantation. Proc Natl Acad Sci USA. 2000; 97:10954–10959. [PubMed: 11005868]

Walkley SU. Secondary accumulation of gangliosides in lysosomal storage disorders. Semin Cell Dev Biol. 2004; 15:433–444. [PubMed: 15207833]

Wandall HH, Pizette S, Pedersen JW, Eichert H, Levery SB, Mandel U, Cohen SM, Clausen H. Egghead and brainiac are essential for glycosphingolipid biosynthesis in vivo. J Biol Chem. 2005; 280:4858–4863. [PubMed: 15611100]

Wing DR, Garner B, Hunnam V, Reinkensmeier G, Andersson U, Harvey DJ, Dwek RA, Platt FM, Butters TD. High-performance liquid chromatography analysis of ganglioside carbohydrates at the picomole level after ceramide glycanase digestion and fluorescent labeling with 2-aminobenzamide. Anal Biochem. 2001; 298:207–217. [PubMed: 11700975]

Wu YP, Proia RL. Deletion of macrophage-inflammatory protein 1 alpha retards neurodegeneration in Sandhoff disease mice. Proc Natl Acad Sci USA. 2004; 101:8425–8430. [PubMed: 15155903]

Wu YP, Mizukami H, Matsuda J, Saito Y, Proia RL, Suzuki K. Apoptosis accompanied by up-regulation of TNF-alpha death pathway genes in the brain of Niemann-Pick type C disease. Mol Genet Metab. 2005; 84:9–17. [PubMed: 15639190]

Yamanaka S, Johnson ON, Norflus F, Boles DJ, Proia RL. Structure and expression of the mouse beta-hexosaminidase genes, Hexa and Hexb. Genomics. 1994; 21:588–596. [PubMed: 7959736]

Yamashita T, Wada R, Sasaki T, Deng C, Bierfreund U, Sandhoff K, Proia RL. A vital role for glycosphingolipid synthesis during development and differentiation. Proc Natl Acad Sci USA. 1999; 96:9142–9147. [PubMed: 10430909]

Yu W, Gong JS, Ko M, Garver WS, Yanagisawa K, Michikawa M. Altered cholesterol metabolism in niemann-pick type c1 mouse brains affects mitochondrial function. J Biol Chem. 2005; 280:11731–11739. [PubMed: 15644330]

Zervas M, Somers KL, Thrall MA, Walkley SU. Critical role for glycosphingolipids in Niemann-Pick disease type C. Curr Biol. 2001; 11:1283–1287. [PubMed: 11525744]

Zhou D, Mattner J, Cantu C 3rd, Schrantz N, Yin N, Gao Y, Sagiv Y, Hudspeth K, Wu YP, Yamashita T, Teneberg S, Wang D, Proia RL, Levery SB, Savage PB, Teyton L, Bendelac A. Lysosomal glycosphingolipid recognition by NKT cells. Science. 2004; 306:1786–1789. [PubMed: 15539565]

Europe PMC Funders Author Manuscripts

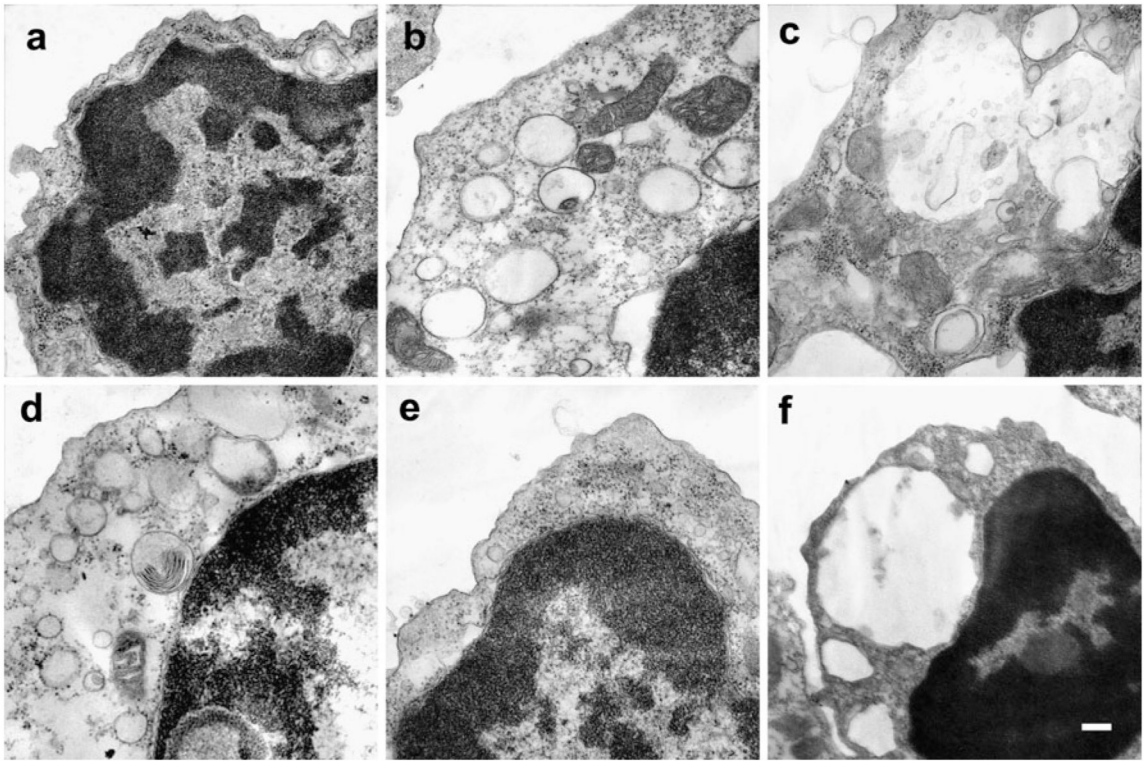

Fig. 1.
Electron microscopy of storing B cells. Representative images of electron dense material accumulating in GSL storage disease B cells. **a** *C57Bl/6*, **b** *α-Gal*$^{-/-}$, **c** *β-Gal*$^{-/-}$, **d** *Hexb*$^{-/-}$, **e** *NPC1*$^{+/+}$, **f** *NPC1*$^{-/-}$. *Scale bar* 0.2 μm

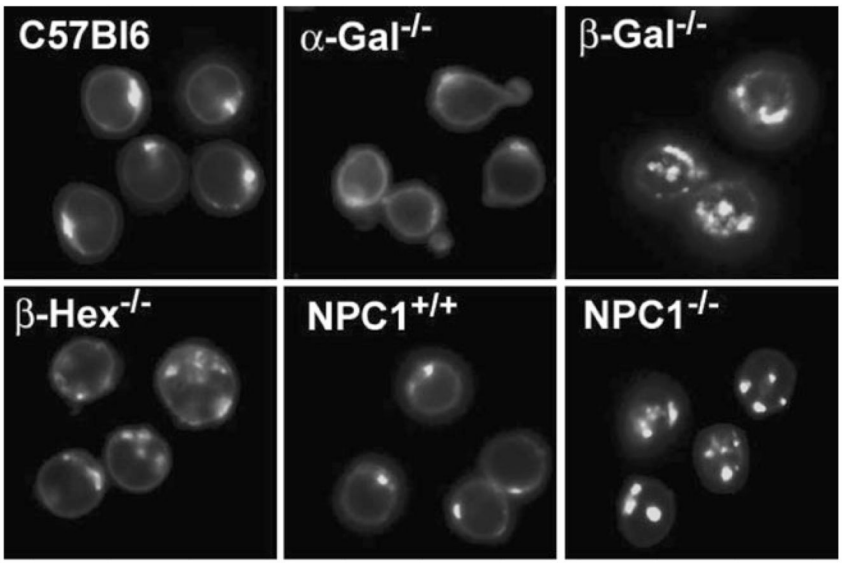

Fig. 2.
Storing B cells show altered BODIPY LacCer trafficking. Representative images of the subcellular localization of BODIPY LacCer. Splenic B cells were isolated and treated with 10 μM BODIPY LacCer in 1% serum for 60 min followed by extensive washing in 10% serum for 5 min and further incubation for 90 min

Europe PMC Funders Author Manuscripts

Europe PMC Funders Author Manuscripts

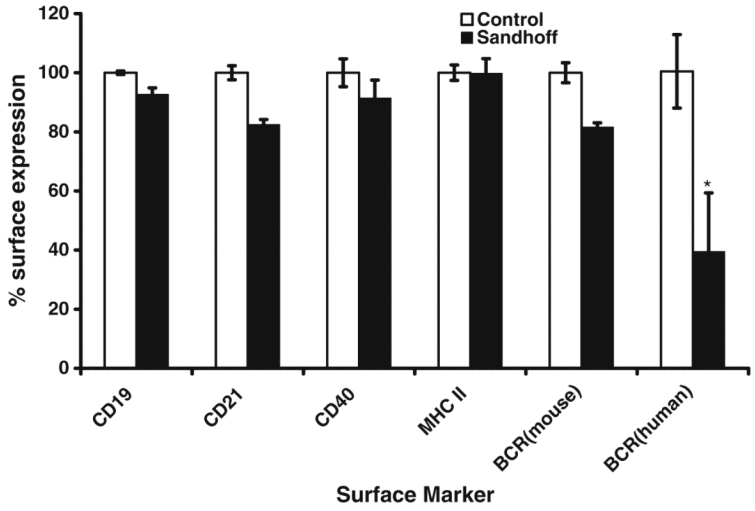

Fig. 3.

BCR receptor and co-receptors are downregulated in *Hexb*$^{-/-}$ (Sandhoff disease) B cells. Spleens of 14-week-old mice were taken to determine the level of expression of CD21, CD19, CD40, MHC II, and sIgM on CD23 high B cells by FACS. A 2-way ANOVA analysis was performed and raft and non-raft components where significantly different, $p<0.05$). The level of expression of sIgG in control and Sandhoff human lymphoblasts were also determined by FACS. *Solid bars* represent Sandhoff B cells. *$p<0.05$

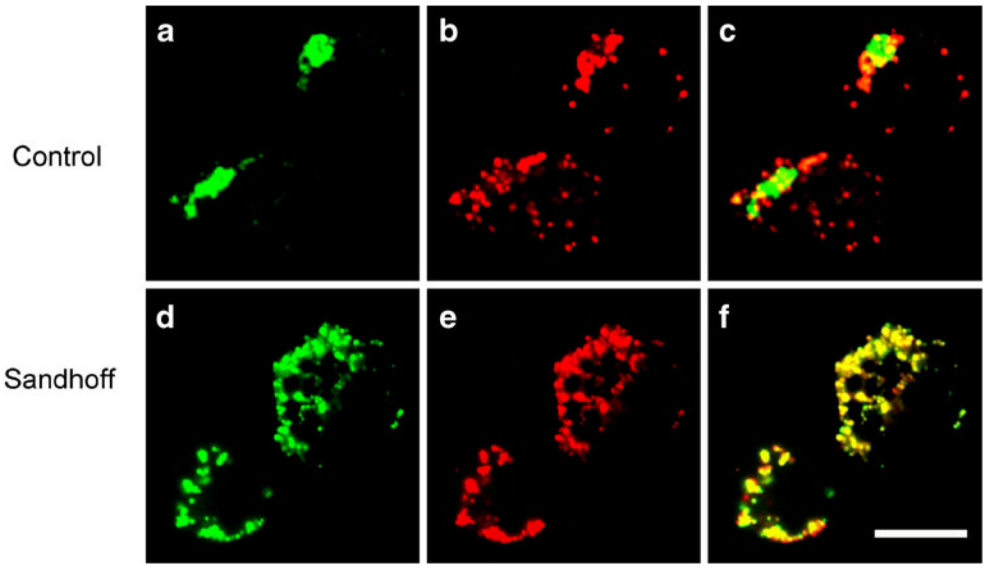

Fig. 4.
Cholera toxin traffics to lysosomes in *Hexb*$^{-/-}$ B lymphoblasts. B lymphoblasts were pulse labeled with fluorescently conjugated cholera toxin (*green*) and lysotracker (*red*). **a–c** Control lymphoblasts, **d–f** Sandhoff lymphoblasts

Europe PMC Funders Author Manuscripts

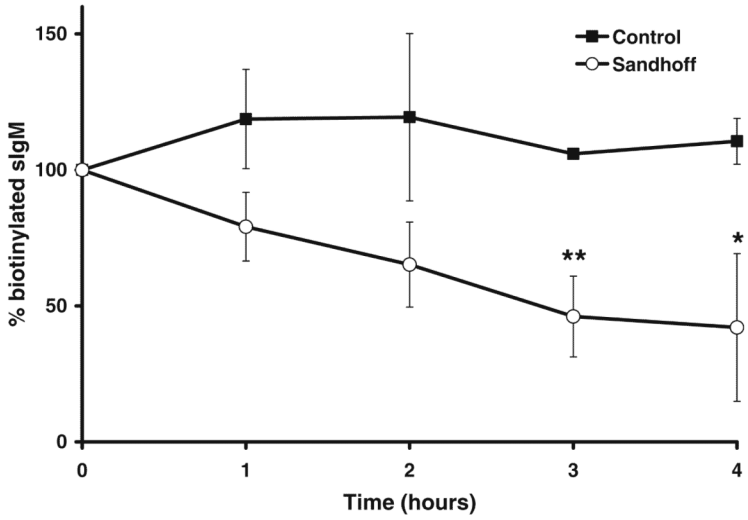

Fig. 5.

BCR receptor shows increased turnover in *Hexb*$^{-/-}$ lymphoblasts. Following pulse labeling with NHS-biotin and immunoprecipitation in the presence of anti-IgM/IgG the half-life of the protein was determined by densitometry. Control (•) *Hexb*$^{-/-}$ (o) *p<0.05, **p<0.01

Europe PMC Funders Author Manuscripts

Europe PMC Funders Author Manuscripts

Table 1

Mouse models used in this study

Mice	Symptom onset (months)	Average life span (months)	Age range analysed (months)
C57Bl/6	None	30	1–12
α-Gal$^{-/-}$	7–12	30	8
β-Gal$^{-/-}$	4–5.5	10	6
β-Hexb$^{-/-}$	2.5	4.5	4
NPC1 $^{-/-}$	1	2.5	1–2

Europe PMC Funders Author Manuscripts

Table 2

B cells isolated from GSL storing mice show disease specific increases in GSLs. Splenocytes were dispersed by gentle disruption between two frosted glass microscope slides, and B cells were isolated using magnetic beads. After GSL extraction and purification, GSLs were digested with ceramide glycanase before derivatisation and quantitation by HPLC. Data are from 4–6 experiments and are expressed as pmol/mg protein ± S.E.

Mouse	LacCer	GA2	Gb3	GM3	GM2	Gb4	GA1	GalNAcGA1	GM1a	GM1b	GD1a
C57B16	280±80	40±l0	70±15	–	40±10	40±10	90±20	30±3	40±9	200±50	240±65
α-Gal$^{-/-}$	180±90	60±35	2,200±560	–	30±10	30±10	90±30	40±10	30±10	190±70	300±90
β-Gal$^{-/-}$	160±80	260±20	120±40	–	70±8	60±30	1,700±200	50±10	110±30	740±100	660±90
β-Hexb$^{-/-}$	360±l00	870±60	50±2	–	90±30	340±50	240±60	30±3	130±40	180±30	260±40
NPC1^{++}	260±40	40±3	30±1	6±1	35±3	30±3	70±6	40±3	20±1	150±20	180±20
NPC1$^{+/-}$	520±200	85±l0	30±3	6±1	50±6	30±5	80±10	35±5	35±5	160±20	190±30
NPC1$^{-/-}$	1,800±450	110±20	140±30	110±3	150±30	160±40	270±60	80±10	70±10	270±40	310±40

LacCer Lactosylceramide, *GA2* GalNAcβ4Galβ4GlcCer, *Gb3* Galα4Galβ4GlcCer, *GM3* Neu5Acα3Galβ4GlcCer, *GM2* GalNAcβ4(Neu5Acα3) Galβ4GlcCer, *Gb4* GalNAcβ4Galα4Galβ4GlcCer, *GA1* Galβ4GalNAcβ4Galβ4GlcCer, *GMla* Galβ3GalNAcβ4(Neu5Acα3)Galβ4GlcCer, *GMlb* Neu5Acα3Galβ3GalNAcβ4Galβ4GlcCer, *GDla* Neu5AcαGalβ3GalNAcβ4(Neu8Acα3)Galβ4GlcCer

Europe PMC Funders Author Manuscripts

Table 3

Total GSL and cholesterol accumulation in storage disease B cells. B cells were purified from splenocytes. After lipid extraction, GSLs were purified by HPLC and cholesterol was quantitated using a microassay. Data are from 4–6 experiments and are expressed as nmol/mg

Mouse	Total GSL	%	Total cholesterol	%
C57Bl6	1.5±0.3	100	60±8	100
α-Gal$^{-/-}$	2.7±0.5	180	110±50	180
β-Gal$^{-/-}$	3.8±0.5	250	160±100	260
β-Hexb$^{-/-}$	3.7±0.5	240	270±90	450
NPC1^{++}	1.3±0.2	100	100±40	160
NPC1$^{+/-}$	1.3±0.2	100	60±20	100
NPC1$^{-/-}$	5.4± 1.3	400	410±100	680

Europe PMC Funders Author Manuscripts

Table 4

Expansion of the lysosomal compartment and changes in GSL endocytosis in storage disease B cells. Lysotracker staining as quantitated by FACS analysis and BODIPY LacCer subcellular location scored as % cells showing a punctate appearance from a total of ~100 cells scored from 5–11 fields

Mouse	Lysotracker (fluorescence/cell Arb units, FACS)	% Punctate (microscopy)
C57B16	300±25	13±3
α-Gal$^{-/-}$	220±98	13±2
β-Gal$^{-/-}$	980±110	73±20
β-Hexb$^{-/-}$	580±53	46±11
NPC1$^{+/+}$	264±76	11±3
NPC1$^{+/-}$	340±200	17±12
NPC1$^{-/-}$	830±130	72±12